Proceedings of the 2017 25th International Conference on Nuclear Engineering
ICONE25
July 2-6, 2017, Shanghai, China

ICONE25-66228

CONTROL SCHEME RESEARCH OF 10MW FLUORIDE SALT COOLED HIGH TEMPERATURE EXPERIMENT REACTOR

Jian Ruan
Shanghai Institute of Applied Physics, CAS
University of Chinese Academy of Sciences, (UCAS)
Shanghai, China, 201800

Yang Zou
Shanghai Institute of Applied Physics, CAS
Shanghai, China, 201800

Minghai Li
Shanghai Institute of Applied Physics, CAS
Shanghai, China, 201800

Hongjie Xu
Shanghai Institute of Applied Physics, CAS
Shanghai, China, 201800

ABSTRACT

Fluoride salt cooled High temperature Reactor (FHR) is a kind of Gen-IV reactor which possesses many attractive features, such as high temperature, low pressure etc. Thermal-hydraulic features of molten salt are different from coolants of traditional reactors, which dominate operation transient behavior of FHR. However, as a new type reactor with sphere fuel element and fluoride salt coolant, FHR has inadequate operating experience and data used for reactor control and the design of power regulating system. Therefore, research of power regulation strategy is very important for FHR in automatic control operation and commercial application.

A code programmed in Fortran platform is used for investigating the system transient behavior, control logic and strategy. Based on the transient analysis code OCFHR for FHR, power control logic strategy is studied on a model of 10 MW Fluoride salt cooled High Temperature Experiment Reactor. OCFHR is a specialized code in FHR transient analysis, which contains point reactor model, simplified core thermal-hydraulic model, molten salt-salt exchanger and molten salt-air exchanger with a tube-shell type, control rod system and power regulation and control model. The control module of OCFHR uses the incremental PID controller to regulate control parameters and adopts the compound mode of control rod adjustment, load adjustment and molten salt flow adjustment, so that it can adjust the control rod position, primary and secondary molten salt flow rate and air flow rate of load at different operating power levels.

Two kinds of steady operation strategies are studied in this paper, which are a) constant outlet coolant temperature and b) constant average coolant temperature. The power level is regulated by control rod while the working temperatures are adjusted by shifting the load with weight coefficients of power and temperature deviations.

The results show that the incremental PID controller with optimized parameters can achieve the control requirement. Both of temperature control strategies gain great performances under 10%FPand 50%FP power regulation. The target power is reached quickly and accurately by using the incremental PID controller while the temperature control is very time-consuming. Compared with b), strategy a) has less temperature overshoot but larger power overshoot and longer adjusting time. The step wise power regulation for FHER is doable when a wide power adjustment range is needed and the simulation 10%FP treated as a step works well. Besides, the preliminary study of varying secondary coolant flow rate also indicates that the secondary loop plays an important part in restraining the deviation of secondary coolant temperatures during the process of balancing the power and load, so it is better to adjust the secondary coolant flow in terms of the power regulation range.

Key words: Control logic, FHR, transient analysis, PID controller.

INTRODUCTION

Fluoride salt-cooled high-temperature reactors (FHRs), which are notable for the coated particle fuel and fluoride salt coolant, provide outstanding priority in electricity generation and process heat applications. Its concept prototype was

developed by Oak Ridge National Laboratory (ORNL), Sandia National Laboratory (SNL) and the University of California at Berkeley (UCB) from 2001 to 2003, assimilating the technical advantages of Molten Salt Reactor (MSR) and High Temperature Reactor (HTR) [1]. Chinese FHR research started at 2012 by TMSR (Thorium Molten Salt Reactor) Group of Chinese Academy of Sciences (CAS), which brought out its own conceptual design of fluoride salt-cooled high-temperature experimental reactor (FHER) [2]. (See Fig.1)

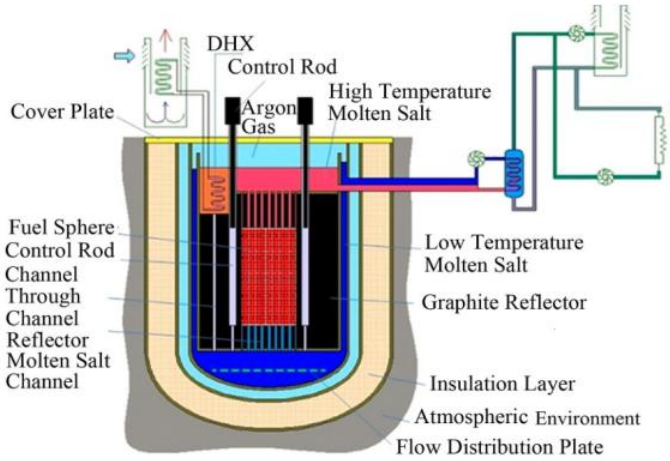

Fig. 1 Schematic diagram of FHER

FHR system possesses some attractive features, such as high temperature, low operation pressure, high power generation efficiency and strong inherent safety. Thermal-hydraulic features of molten salt are different from coolants of other reactors, which dominate operation transient behavior of FHR. The coolant in primary loop is FLiBe (2LiF-BeF2) which has low neutron absorption cross-section, large heat capacity (~2400J/(kg•°C)), a rather wide range of liquid-phase temperature between 450 and 1400°C, providing an abundant temperature safety margin[3]. FLiBe allows FHRs to increase average power density, decrease maximum pressure tolerance of material and enhance spatial compactness. The fuel element consists of a fuel core (either in plate type or spherical type) and several shielding materials outside the core (see Fig.2). The fuel core is mainly made up of tristructural-isotropic (TRISO),providing several hundred degrees safety margin comparing to rated operational temperature and leaving little possibility for fission products to leak out[4].In this paper, only spherical pebble type fuel element is considered.

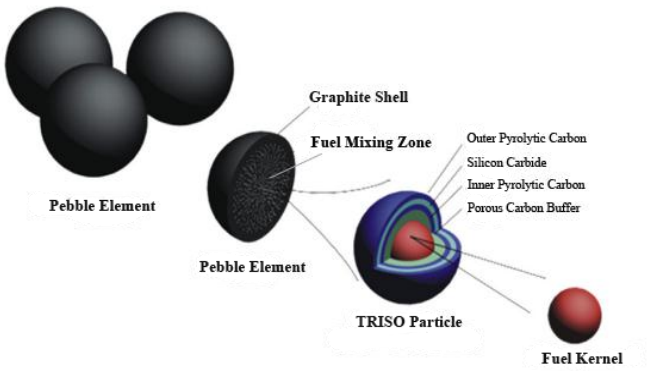

Fig. 2 Diagram of pebble element

The understanding of transient performances is significant in FHRs design, for the large heat capacity of salt may extend transient response time and the multilayered structure of fuel element means non-negligible temperature variation delay cannot reflect the change of fuel temperature quickly. Moreover, the salt flow channels, pipelines and other large components can also restrain the thermal transfer speed as it costs no less than 70s for coolant to flow across the main loop, resulting in obviously delaying in transient variations when disturbances occurs or power adjusts. Besides, FHR has inadequate operating experience and data used for reactor control and the design of power regulating system, and the characteristics of FHR make it hard to refer mature light water reactors' control strategies. Therefore, research of power regulation strategy is vital for FHR in automatic control operation and commercial application.

Analysis of transient operation and control scheme is often researched by experiment and simulations. A great deal of work about reactor control logic and strategy has also been researched so far. Chen employs MATLAB platform to analyze the transient performances of an FHR coupled with a helium Brayton power cycle [5]. Ablay uses a modeling and control approach to study the power conversion performance of advanced nuclear plants with gas turbines [6]. Chu uses an analytical method to design PID controller for the power control system of an experiment reactor, and compares the performance of some control models [7]. Shi studies the control scheme of 10MW high temperature gas-cooled reactor, researches three kinds of control strategies and concludes that using main water pump to adjust the steam temperature and helium blower to keep the helium flow proportional with nuclear power can solve coupled control problem of loops of HTGR[8].

In this paper, the OCFHR is developed to study operation transient behaviors of FHRs and will be simply introduced with the FHER model in the following section. After that, two kinds of steady operation strategies are studied and a control scheme of FHER is offered after simulations and analysis.

MODEL AND METHOD

OCFHR Model

OCFHR (Operation and Control of FHR) is developed for researching operation control strategy of FHR. This code contains some calculation models like point reactor model, reactivity feedback model, simplified thermal-hydraulic model, and power level control model.

The point reactor model is based on the fifteen-group point kinetic equations due to the existence of beryllium [9]. Therefore among the fifteen delayed-neutron precursor groups, nine groups are added in due to the photo-neutron emission, this could enlarge neutron lifetime and increase the effects of delayed neutrons. The equations are shown as follows:

$$\frac{dn(t)}{dt} = \frac{R(t)-\beta}{l}n(t) + \sum_{i=1}^{15}\lambda_i C_i(t)$$
$$\frac{dC_i(t)}{dt} = \frac{\beta_i}{l}n(t) - \lambda_i C_i(t) \quad (1)$$

where n is the neutron density [n/m^3]; C is the concentration of neutron precursor; β is the total delayed neutron fraction;$\beta_i$is the ith delayed neutron fraction;$\lambda$is the decay constant [s^{-1}]; $l$is the mean neutron generation time [s]. $\beta$and λaregained from neutron physics calculation.

The reactivity feedback model includes several parts. Fuel reactivity coefficient is negative due to the Doppler Effect, and the primary coolant temperature reactivity coefficient is also negative because of its neutron property. Besides, the control rod effect is also important for reactivity control in most FHR designs. Therefore, OCFHR combines these items to the reactivity item ρ in the correlation.

$$R(t) = \rho_0 + \rho_{rd} + \alpha_{fg}\Delta\bar{T}_{fg} + \alpha_s\Delta\bar{T}_s + \alpha_{ge}\Delta\bar{T}_{ge} \quad (2)$$

where $\rho_0$is the initial reactivity; $\rho_{rd}$is the control rod reactivity; $\alpha_{fg}$is the mixing zone reactivity coefficient; $\alpha_s$is the primary coolant reactivity coefficient; $\alpha_{ge}$is the graphite reflector reactivity coefficient; $\Delta\bar{T}_{fg}, \Delta\bar{T}_s, \Delta\bar{T}_{ge}$are mixing zone, primary coolant and reflector mean temperature variations respectively [°C].

FHER's system employs three loops and many components, such as pebble bed, cavities, pipes, pumps, channels, IHX (intermediate heat exchanger), SHX (secondary heat exchanger) and an air radiator as load. OCFHR is based on lumped parameter method, which axially divides the object structure into several independent nodes and each node represents segmental geometrical and physical parameters of original structure. Then differential equations can be developed within and between every single and adjacent nodes including material properties, heat transfer and conservation equations. Besides, every component of FHER is labeled by a unique series of numbers, where each number denotes a node. Hence, the whole system can be simplified under this modularization thinking, which brings in significant improvement in modeling speed [10]. Fig.3 and Fig.4 show the node diagram and simplifications of FHER, relevant parameters of it are shown in table 1, 2 and 3.

The mass conservation in one fluid node conforms to that mass flow rate at the outlet equals to that at the inlet. The one-dimensional form is shown as follows.

$$\frac{\partial\rho}{\partial t} + \frac{\partial\rho u}{\partial x} = 0 \quad (3)$$

where ρ is the density of coolant [kg/m3]; u is the average flow rate of coolant on x-dimension[m/s];

The coolant is driven by a hypothetical pump, which offers the pressure head to compensate the friction pressure drop and form pressure drop and gravitation pressure drop.

$$\frac{\partial W}{\partial t} + \frac{\partial}{\partial x}\left(\frac{W^2}{\rho A}\right) + \frac{fW^2}{2\rho DA} + \frac{KW^2}{2\rho A} = \frac{\partial P}{\partial x} \quad (4)$$

where W is mass flow rate of coolant [kg/s]; f is the factor of friction pressure drop, K is the factor of form pressure drop, P is pressure head of pump.

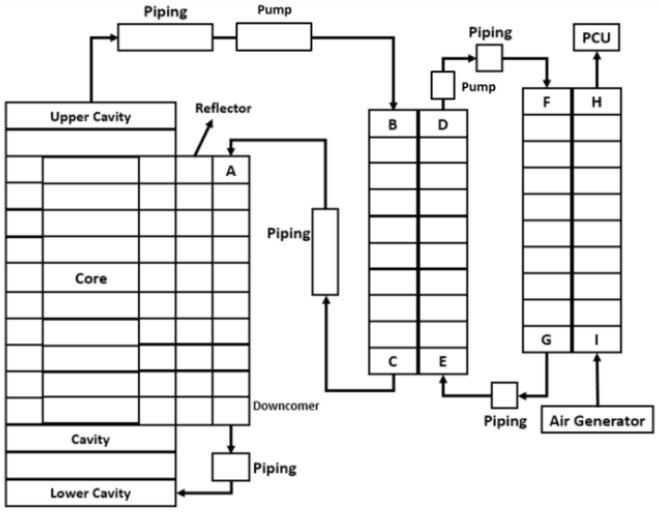

Fig. 3 Node diagram of FHER

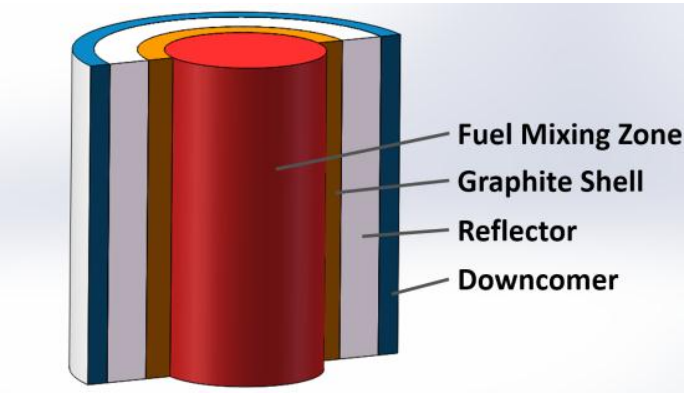

Fig. 4 Simplifications of Pebble bed

OCFHR employs some simplifications and equivalences to model specific geometry. The core contains more than ten thousand pebbles and each pebble has thousands of TRISO particles, so it is impossible to model without compromise. OCFHR firstly divides the pebble bed into two areas: cylindrical graphite shell and cylindrical fuel mixing zone, while the latter contains TRISO particles and graphite moderator. Secondly, some parameters are acquired from neutron physics program such as temperature reactivity coefficients, decay constants and portions of neutron precursors. Besides, heat transfer calculation of the core is solved by using the mature porous medium Wakao correlation due to the impractical calculation of heat transfer between pebble bed and salt coolant [11].

$$\mathrm{Nu} = 2.0 + 1.1 * Re_D^{0.6} Pr^{1/3} \qquad (5)$$

where Nu, Re and Pr represent the Nusselt number, Reynolds number, and Prandtl number, respectively; D is the equivalent diameter; the correlation is applicable for 15<Re<8500.

For the pressure drop in the core, the equation used is the Ergun equation which is suitable for porous medium [12]:

$$\frac{\Delta P_c}{L} = -\frac{150\mu}{D_p^2}\frac{(1-\varepsilon)^2}{\varepsilon^3}u_i - \frac{1.75\rho}{D_p}\frac{(1-\varepsilon)}{\varepsilon^3}|u|u_i \quad (6)$$

where ΔP_c, ε, μ, D_p, L are the core pressure drop, volume fraction, viscosity, pebble diameter, and the height of pebble bed, respectively.

Table 1. FHER geometric and steady-state operating parameters

Parameter	Unit	Value
Total thermal power	MW	10.0
Primary coolant inlet temperature	°C	672.0
Primary coolant outlet temperature	°C	700.0
Primary coolant mass flow rate	kg/s	150.0
Fuel mixing zone temperature coefficient of reactivity	pcm/°C	-5.69
Salt temperature coefficient of reactivity	pcm/°C	-2.27
Graphite temperature coefficient of reactivity	pcm/°C	0.74
Secondary coolant mass flow rate	kg/s	260.0
Secondary coolant inlet temperature	°C	610.0
Secondary coolant outlet temperature	°C	630.0
Air fan mass flow rate	kg/s	51.0

Table 2. Node Temperatures at rated operation state

Parameter	Unit	Value
A: Inlet of Downcomer	°C	672.0
B: Inlet of IHX hot side	°C	700.0
C: Outlet of IHX hot side	°C	672.0
D: Outlet of IHX cold side	°C	630.0
E: Inlet of IHX cold side	°C	610.0
F: Inlet of SHX hot side	°C	630.0
G: Outlet of SHX hot side	°C	610.0
H: Outlet of SHX cold side	°C	227.0
I: Inlet of SHX cold side	°C	40.0

Table 3. FHER geometric structure parameters

Parameter	Unit	Value
Fuel pebble diameter	cm	6.00
Fuel pebble number	-	10855
Graphite shell thickness	cm	1.00
TRISO particles in one pebble	-	10000
Diameters of TRISO inner layers(from core to shell)	μm	250/430/ 500/580
Active zone cylinder diameter	m	1.35
Active zone cylinder height	m	1.30
Active zone volume	m^3	2.76
Upper reflector volume	m^3	0.72
Lower reflector volume	m^3	0.63
Upper plenum volume	m^3	0.64
Lower plenum volume	m^3	0.27
Diameter of pipe	m	0.126
Length of hot leg	m	10.0
Length of cold leg	m	10.0
Reflector diameter	m	2.85
Reflector height	m	3.00
Total length of secondary loop	m	20.0
FLiBe volume in IHX	m^3	0.64
FLiNaK volume in IHX	m^3	1.35
FLiNaK volume in SHX	m^3	0.70

OCFHR adopts incremental PID controller to adjust the power level, coolant temperature and load. This method takes error of regulated variable as input and the place increment of controller as output instead of the actual place of controller. So it can use an integrator to memorize the actual place of regulator and lead little impact when the regulator fails. Equation (7) and (8) are forms of typical and incremental PID controller. The PID parameters used in OCFHR are gained from the combination of experience and attenuation curve tuning rules. The detailed optimization of PID controller parameters is not introduced here [13].

$$\mathrm{u(t)} = \mathrm{K_p}\left[\mathrm{e(t)} + \frac{1}{\mathrm{T_i}}\int_0^{\mathrm{t}} \mathrm{e(t)dt} + \mathrm{T_d}\frac{\mathrm{de(t)}}{\mathrm{dt}}\right] \quad (7)$$

$$\Delta\mathrm{u(k)} = \mathrm{u(k)} - \mathrm{u(k-1)} = \mathrm{K_p}\Delta\mathrm{e(k)} + \mathrm{K_i}\Delta\mathrm{e(k)} + \mathrm{K_d}\big(\Delta\mathrm{e(k)} - \Delta\mathrm{e(k-1)}\big) \quad (8)$$

$$\Delta\mathrm{e(k)} = \mathrm{e(k)} - \mathrm{e(k-1)} \quad (9)$$

Using equation (8) and (9), the form in the model is as follows:

$$\Delta u(k) = Ae_k - Be_{k-1} + Ce_{k-2} \quad (10)$$

where K_p, K_i and K_d mean proportional factor, integrate factor and differential factor, respectively, while A, B and C are new PID factors after being simplified. $e(k)$ represents the k-th error of regulated variable between its sampling value and aim value. $\Delta u(k)$ is the k-th inserting speed of control rod reactivity which varies between-5pcm/s and 5pcm/s which can also be converted to rod shifting.

In OCFHR, other regulation method also exists such as linear adjustment, polynomial adjustment, and a fuzzy controller also works for regulating power and temperature. In this paper, only the PID controller and simple adjustment methods are considered.

Control strategy and logic

Typical reactor operation modes separate to two parts: base load mode and load follow mode. The former is better for FHER because the power regulation system for an experiment reactor can be simpler with the absence of electricity system that could reduce thermal shock to generating equipment and extend their operation life. Steady operation logic demands the reactor power to operate at the setting and also to keep some parameters like temperature, pressure and coolant flow working in a reasonable range stably. Considering of the high and low temperature safety limitations of FHER, a temperature control system is required.

Traditional temperature steady regulating strategies includes: constant coolant temperature at core outlet and constant coolant average temperature of core. When adjusting power level, the first strategy will not lead violent thermal shocks to components and fuel elements which can prolong their operation time and lower fuel damage rate. However, the later one is more flexible with many optional temperature working points and advantageous to promote the self-stabilization ability of FHR. Compared with the temperature adjustment strategies which treat power level and coolant temperature with equal importance, power control is also remarkable by using control rod, while the temperature regulation lies in load adjustment. This paper analyzes these methods and researches their performances in order to make reasonable control logic for FHR. Table 4 shows the temperature control strategies and Figure 5 is the flow-process diagram of strategy b).

Table 4. Classification of temperature control strategies of FHER in OCFHR

Strategy List
a) Constant outlet coolant temperature strategy
b) Constant average coolant temperature strategy

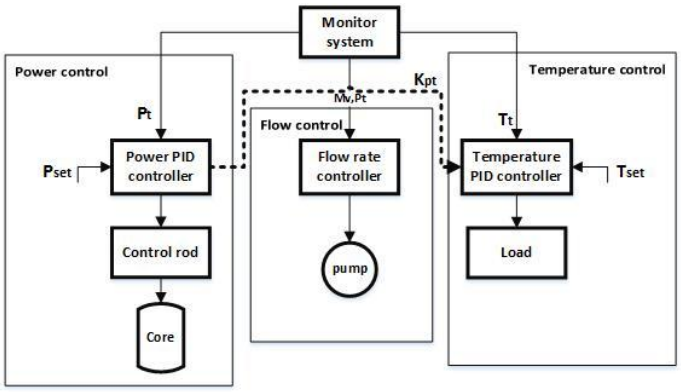

Fig. 5 Structural representation of control scheme

where P_{set}, P_t, T_{set}, T_t, M_v and K_{pt} are the power and primary coolant temperature setting values and measured values, present coolant mass flow rate and a gain provided from power PID controller to temperature controller.

Fig. 5 shows the structural representation of control scheme in OCFHR. This scheme contains three parts: the left part is power control, the middle is flow rate control and the last is temperature control. The power control is realized by control rod which is regulated by a PID controller. The temperature controller acquires the error of controlled variable and a coefficient from power controller, so the load adjustment can be approximately synchronous with the power to reduce temperature departure. The flow control is a preliminary part for researching the influence of flow variation, and it does affect the control performance during the process of balancing power and load.

Control rod adjustment can change the power quickly so it needs the PID controller to calculate appropriate speed and total shifting to make controlled variable reach its target. Simultaneously, it also affects coolant temperature. Thus the load regulation is acquired to adjust the operating coolant temperature, but it will costs plenty of time due to the three

loop arrangement and large heat inert of salt. Besides, adjusting the primary coolant mass flow can also influence the coolant temperature which is already used in HTGR and SFR [14]. Mass flow of coolant is usually in direct proportion to present power level. The rising flow rate can carry off more heat from fuel when power needs to be increased, so positive reactivity is inserted. However, this adjustment should be implemented after doing a great deal of experiments and simulation researches, and there is not an insightful research of the proportion parameter here.

$$\frac{P_t}{P_{rated}} = \frac{\dot{m}_t}{\dot{m}_{rated}} \qquad (11)$$

where P_t,$\dot{m}_t$,P_{rated} and $\dot{m}_{rated}$ are the present and rated power and coolant flow rate respectively.

In this paper, the operation strategies above are introduced to the control module of OCFHR to testify their performance on FHER while the operation mode is just the base load mode. After simulations and comparisons, a set of control logic and strategies are proposed to guide FHR's operation.

SIMULATION

A rated operation state of FHER is adjusted in OCFHR before each simulation.

Constant outlet coolant temperature strategy

This section studies the strategy a), which is advantageous for bringing out small thermal shocks to posterior components. In this case, the target power is 9MW with a dead zone of 0.01MW and the temperature of coolant at core outlet is set at 700℃ with an allowable fluctuation of 2℃.

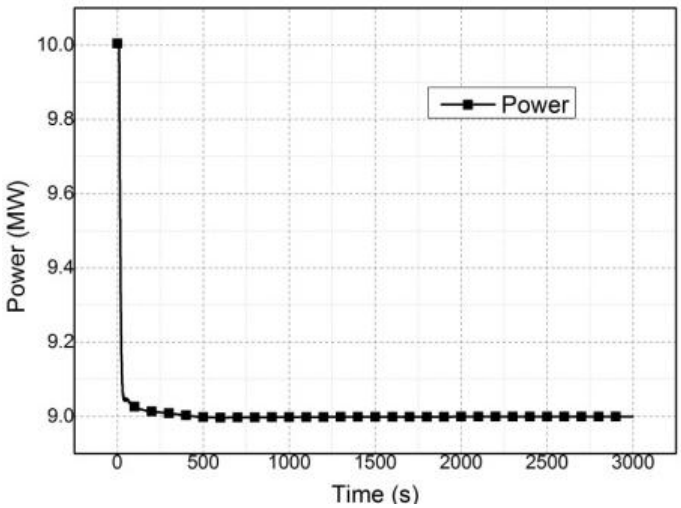

Fig. 6 Reactor power evolution of strategy a)

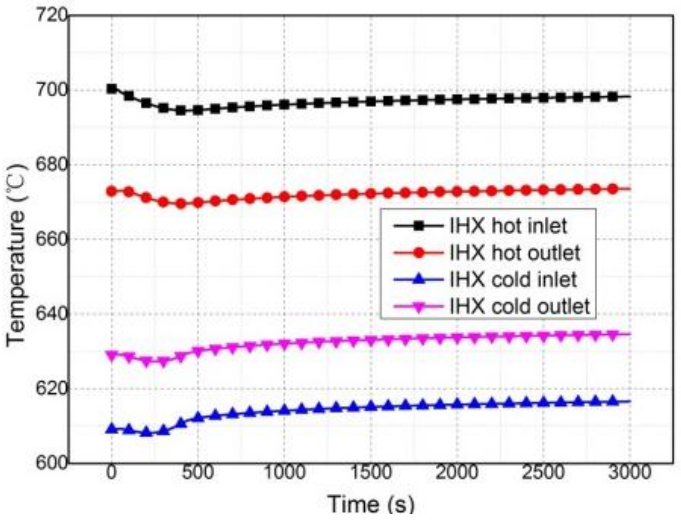

Fig. 7 Temperature variations of coolants of strategy a)

Fig.6 and 7 depicts the control performance of power decrease of 10%FP. The power regulation is quick and accurate by using the incremental PID controller, and this process costs about 300s with an overshoot of 0.001MW. The temperature control is obviously slow which reaches to the target zone at about 1600s, and the maximum temperature deviation of the coolant at outlet is 5.5℃.The temperature variations of primary coolant at IHX inlet and outlet are -0.6 and 2.1 respectively.

From the graphs above, the temperature control of primary coolant is quite inertial because the three loops of FHER cost much time for heat transferring and the property of salt also plays a part to prolonging this process. Reactor power regulation is often handled with step jumping method, which separates a large power adjustment range to several small steps. This can help operators to acquire real-time parameters of reactors at some time in order to diagnose its state and also to adjust the temperature point back to the setting. The temperature control is important for FHER which has safety limits at higher temperature and lower point. Therefore, stepwise power regulation for FHER is a necessity and 10%FP as a step is acceptable.

Constant average temperature strategy

This strategy permits temperature drifting within a reasonable range, which reduces the frequency of load shifting and adjustment time. The target power of the case is 9MW with a dead zone of 0.01MW, and the average temperature of coolant in core is set at 687℃ with an allowable fluctuation of 2℃.

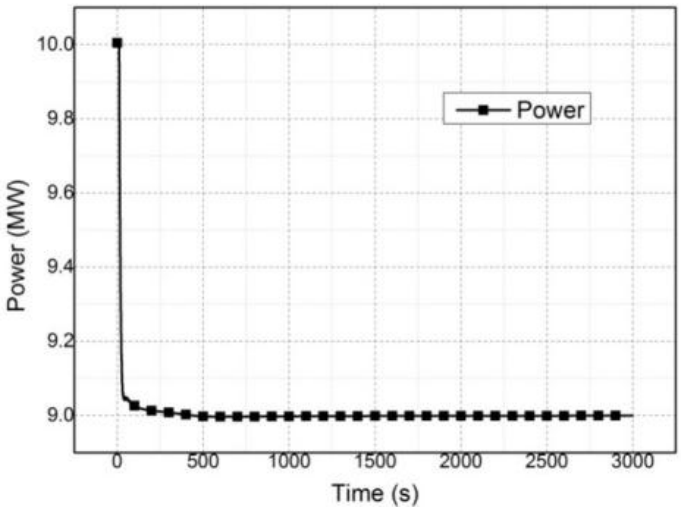

Fig. 8 Reactor power evolution of strategy b)

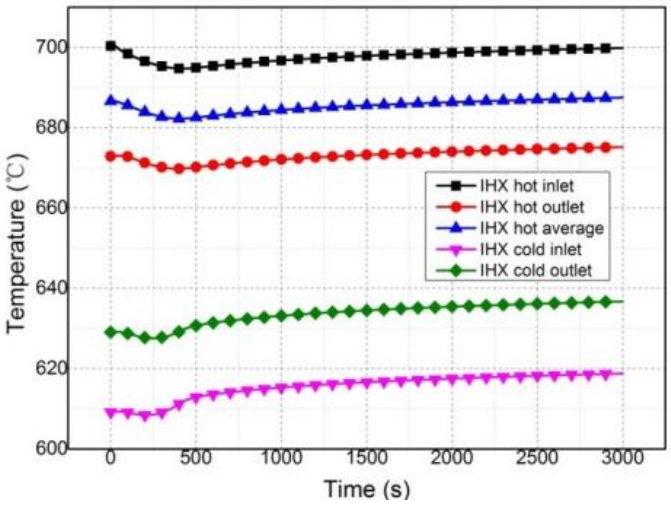

Fig. 9 Temperature variations of coolants of strategy b)

Fig. 8 gives the power control performance by PID controller, and the power reaches to the dead zone at about 270s. Fig.9 shows the effects of constant average coolant temperature strategy. At first, the average value decreases with the power level, then it begins to bounce back to the setting point and arrives at steady state at 1500s by adjusting load. The overshoot of power is 0.002MW, and the maximum average temperature deviation of primary coolant is 4.7℃ while that deviations of inlet and outlet at 1500s are-0.5℃ and 2.3℃ respectively.

Compared with the strategy a), strategy b) needs less time to return to the settings. Neither beneficial nor harmful, this strategy allows the existence of many steady operation temperature points, although the highest and lowest temperatures of primary coolant during the process are also limited in an acceptable zone.

Wide range power adjustment

The power sometimes is needed to be increased or decreased in a wide range, so the process will be rather time-consuming. Therefore, a simulation of wide range power adjustment is studied to testify the performance of the control scheme. The target power of the case is 5MW with an dead zone of 0.01MW, and the temperature of coolant at core outlet is set at 700℃ for strategy a) while the average temperature is set at 687℃ for strategy b). Both strategies are with same tolerable fluctuation of 2℃.

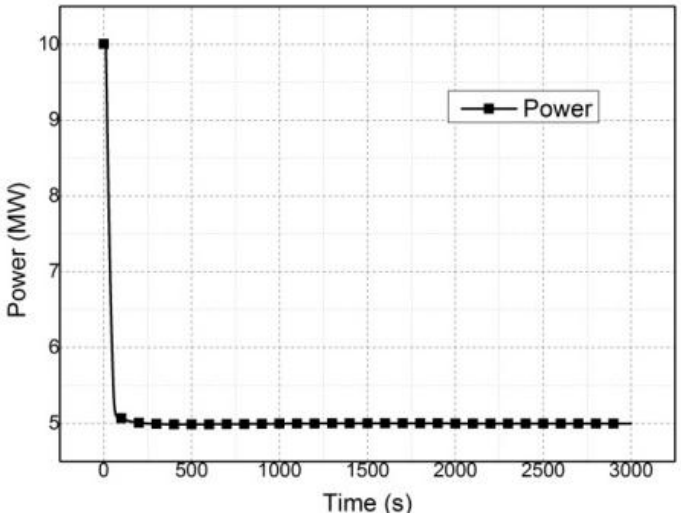

Fig.10 Power variation of strategy a)

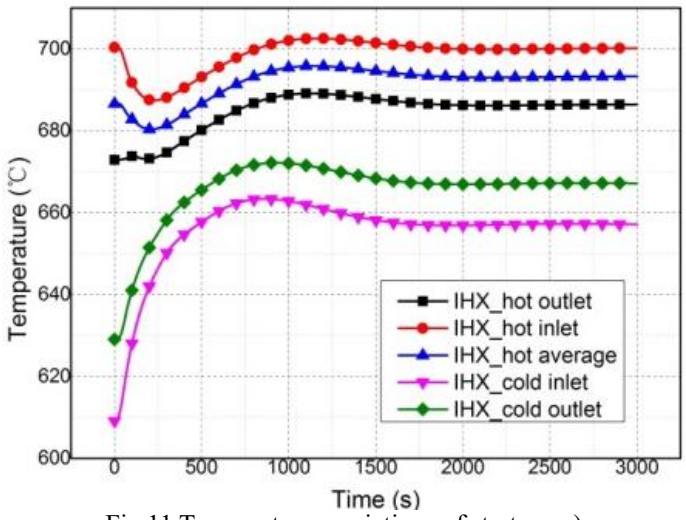

Fig.11 Temperatures variations of strategy a)

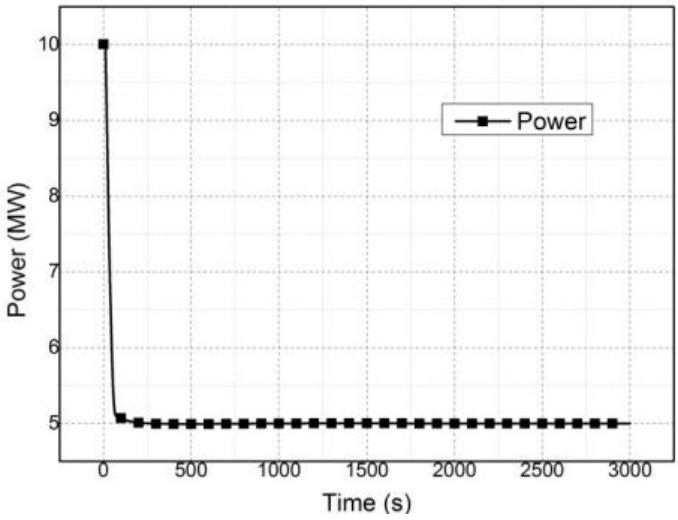

Fig.12 Power variation of strategy b)

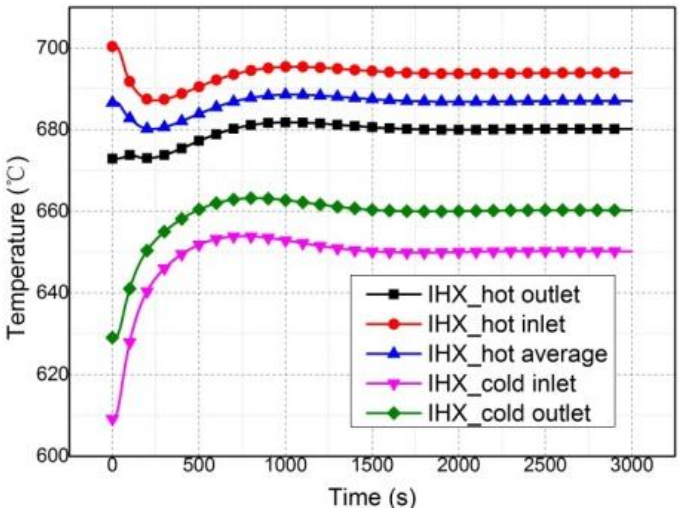

Fig.13 Temperatures variations of strategy b)

Fig 10 to 13 depicts the power and coolant temperatures variations of strategy a) and b). They both gain good power adjustment performance regulated by PID controller. The overshoots in a) and b) are 0.012MW and 0.009MW and the maximum deviations of controlled temperature variables of two strategies are 12.5℃ and 16℃, respectively. However, strategy b) spends less time than a) to reaching to the dead zone and steady state.

One serious thing occurs that the coolant temperatures of secondary loop in a) and b) both increase rapidly and deviates seriously from their original operating points. This is because power and load are adjusted quickly to meet their control target while the heat is blocked in the secondary loop. Meanwhile, large temperature change can affect the capability of equipment in this loop and lower their operation life. Therefore some measures should be executed to deal with this consequence. According to the coolant flow adjustment of HTGR and SFR, a preliminary simulation that regulating the coolant flow rate is carried on.

Secondary coolant flow varies against the wide range power adjustment

From sections above, the temperatures of secondary coolant do not change in a big extent, but the effect will be extrusive under a wide range power adjustment. This part studies the performance of strategy b) by adjusting secondary coolant flow rate and analyzes its consequence.

The target power level is set at 5MW at the 10s and the secondary coolant flow rate varies proportionally to the power level. This simulation possesses two cases: case 1 keeps that flow constant; case 2 acts as a control group to adjust the secondary coolant flow rate.

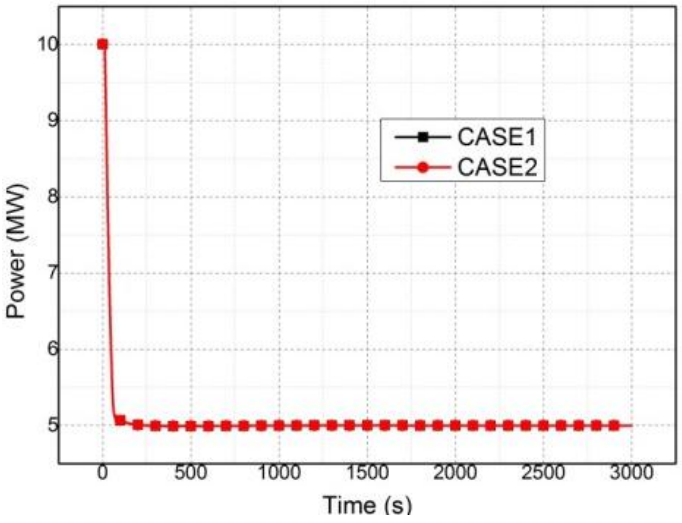

Fig. 14 power evolution of 50%FP in two cases

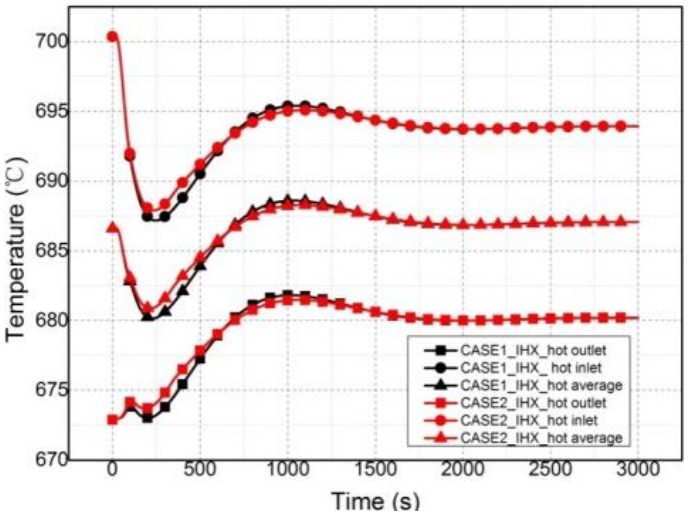

Fig. 15 Temperature variations of primary coolants in two cases

Fig.14 shows the power decrease of two cases. Though the control of secondary coolant mass flow in two cases is different, the power varies with little divergence due to the effect of control rod. The max power overshoot of the two cases is 0.008MW and adjustment time is about 250s, while the time length of changing flow rate in case 2 is 300s.

Fig.15 and 16 depict the variations of coolant temperatures in primary and secondary loops of two cases. In case 1, the variations of primary coolant temperatures at inlet and outlet of IHX are 7.3℃ and -6.7℃ while those of secondary coolant at inlet and outlet of SHX are 41.8℃ and 31.2℃, respectively. In the control group, the variations at steady state of primary coolant temperatures at inlet and outlet of IHX equals to those of case 1 while those of secondary coolant at inlet and outlet of SHX are 26.2℃ and26.5℃, respectively. The temperature difference of secondary coolant in case1 is half of that in case 2 due to the change of mass flow rate.

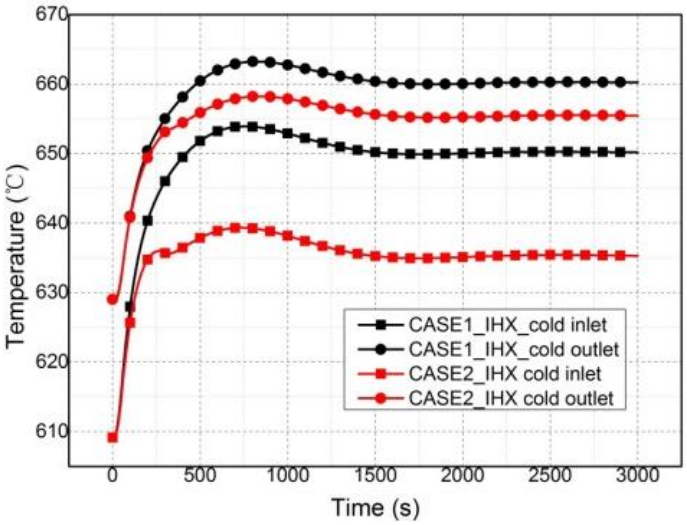

Fig. 16 Temperature variations of secondary coolants in two cases

In FHER, the secondary loop takes the duty to prevent primary salt from leaking out and also acts as an absorber of tritium, but it indeed affects heat transfer of FHER. If the secondary coolant mass flow keeps constant, it becomes a thermal absorber which stores the heat coming from the unbalance of power and load. Therefore, changing secondary coolant mass flow rate can help to decrease the operating point of the secondary loop, especially for wide power range adjustment. Besides, the control scheme of constant average coolant temperature is viable no matter how the regulation range is.

CONCLUSION

This research analyzes two possible control schemes of FHER and simulates their performances on power adjustment and primary coolant temperature maintenance. From the results obtained, both of the temperature control strategies gains great performances under 10%FPand 50%FP power regulation. The target power is reached quickly and accurately by using the incremental PID controller while the temperature control is very time-consuming. Compared with b), strategy a) has less temperature overshoot but larger power overshoot and longer adjusting time. According to the 10%FP simulations, the step jumping method of power adjustment is acceptable.

Besides, the temperatures of secondary coolant vary obviously when the power is widely regulated, and the preliminary simulation indicates that flow rate control can ease the effects of operating point drifting. Further, the optimizations of parameters in these control schemes will be studied in the continuous work.

ACKNOWLEDGMENTS

This research is being studied using funding received from the Shanghai Institute of Applied Physics(SINAP) of Chinese Academy of Sciences' Strategic Priority Program(Award number : XDA02010200) .

NOMENCLATURE

C the concentration of neutron precursor
$e(k)$ the k-th error of regulated variable between its sampling value and aim value.
ΔP_c the active zone pressure drop
$\Delta u(k)$ the k-th inserting speed
D_p pebble diameter
K_p mean proportional factor
K_i integrate factor
K_d differential factor
L height of pebble bed
n the neutron density
Nu the Nusselt number
Pr Prandtl number
Re Reynolds number
$\Delta\bar{T}_{fg}$ mean temperature variations
u the average flow rate of coolant on x-dimension
α_{fg} the mixing zone reactivity coefficient
α_s the primary coolant reactivity coefficient
α_{ge} the graphite reflector reactivity coefficient
ε volume fraction
μ viscosity of coolant
β the total delayed neutron fraction
λ the decay constant
l the mean neutron generation time
ρ the density of coolant
ρ_0 the initial reactivity
ρ_{rd} the control rod reactivity

REFERENCES

[1] Forsberg. CW. 2005. The advanced high-temperature reactor: high-temperature fuel, liquid salt coolant, and liquid-metal reactor plant. Prog.Nucl.Energy 47(1-4), 32-43 (2005).DOI: 10.1016/j.pnucene.2005.05.002.

[2] TMSR center. Pre-conceptual design of a 2MW Pebble bed Fluoride Salt Coolant High Temperature Test Reactor. Shanghai Institute of Applied Physics (2012).

[3] D.F. Williams et al. Assessment of Candidate Molten Salt Coolants for the Advanced High-Temperature Reactor(AHTR). ORNL-TM-2006-12 U.S. Department of energy (2006).DOI: 10.2172/885975.

[4] Andrade et al. Technical Description of the "Mark 1" Pebble-Bed Fluoride-salt-Cooled High-Temperature Reactor (PB-FHR) Power Plant. UCBTH-14-002.Department of Nuclear Engineering, University of California, Berkeley (2014).DOI: 10.13140/RG.2.1.4915.7524.

[5] Minghui Chen et al. Transient analysis of an FHR coupled to a helium Brayton power cycle. Prog.Nucl.Energy 83, 283-293 (2015).DOI: 10.1016/j.pnucene.2015.02.015.

[6] Günyaz Ablay. A modeling and control approach to advanced nuclear power plants with gas turbines. Energy Conversion and Management 76,899-909(2013). DOI:10.1016/j.enconman.2013.08.048.

[7]Xinyuan Zhu et al. Analytical design method of PID controller for experimental reactor power control system. Atomic Energy Science and technology38(1):65-69(2004).

[8] Lei Shiet al. Control Scheme Research of 10MW High Temperature Gas-Cooled Reactor. Nuclear Power Engineering 22(5):392-395(2001).

[9] S.S.Lomakin, Yu. A. Nechaev. Transient processes and the measurement of reactivity of a reactor containing Beryllium. Translated from Atom nayaEnergiya.Vol 18.No.1, January, 33-40 (1965). DOI: 10.1007/BF01116353.

[10] Mark R. Galvin. System Model of a Natural Circulation Integral Test Facility. OregonState University (2009).

[11] N. Wakao et al. Effect of Fluid Dispersion coefficients on Particle-to-Fluid heat transfer coefficients in Packed Beds. Chemical Engineering Sci. 34, 325-336 (1978).DOI: 10.1016/0009-2509(79)85064-2.

[12] Ergun S. Fluid Flow Through Packed Columns. AIChE J, 18(2):361-371(1972).

[13] Kangling Fang et al. Process Control System. Wuhan:Wuhan University of Technology Press,69-100(2009)

[14] Houming Zhang, Tianying Duan et al. Study on the simulation operation of pool type sodium cooled fast reactor power plant. NuclSciEng: 31(1):28-40(2011).